

## UC Davis

### UC Davis Previously Published Works

**Title**

Microfluidic generation of alginate microgels for the controlled delivery of lentivectors

**Permalink**

<https://escholarship.org/uc/item/3z523978>

**Journal**

Journal of Materials Chemistry B, 4(43)

**ISSN**

2050-750X

**Authors**

Madrigal, Justin L  
Stilhano, Roberta S  
Siltanen, Christian  
et al.

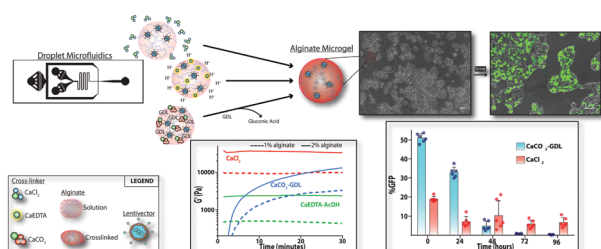
**Publication Date**

2016-11-21

**DOI**

10.1039/c6tb02150f

Peer reviewed



### Microfluidic generation of alginate microgels for the controlled delivery of lentivectors

Justin L. Madrigal, Roberta S. Stilhano, Christian Siltanen, Kimberly Tanaka, Sabah Rezvani, Ryan Morgan, Alexander Revzin, Sang W. Han and Eduardo A. Silva\*

Microgels fabricated through distinct microfluidic procedures encapsulate and release functioning lentivectors in a controlled manner.

Please check this proof carefully. **Our staff will not read it in detail after you have returned it.**

Translation errors between word-processor files and typesetting systems can occur so the whole proof needs to be read. Please pay particular attention to: tabulated material; equations; numerical data; figures and graphics; and references. If you have not already indicated the corresponding author(s) please mark their name(s) with an asterisk. Please e-mail a list of corrections or the PDF with electronic notes attached – do not change the text within the PDF file or send a revised manuscript. Corrections at this stage should be minor and not involve extensive changes. All corrections must be sent at the same time.

**Please bear in mind that minor layout improvements, e.g. in line breaking, table widths and graphic placement, are routinely applied to the final version.**

Please note that, in the typefaces we use, an italic vee looks like this: *v*, and a Greek nu looks like this:  $\nu$ .

We will publish articles on the web as soon as possible after receiving your corrections; **no late corrections will be made.**

Please return your **final** corrections, where possible within **48 hours** of receipt, by e-mail to: materialsB@rsc.org

## Queries for the attention of the authors

Journal: **Journal of Materials Chemistry B**

Paper: **c6tb02150f**

Title: **Microfluidic generation of alginate microgels for the controlled delivery of lentivectors**

Editor's queries are marked on your proof like this **Q1**, **Q2**, etc. and for your convenience line numbers are indicated like this 5, 10, 15, ...

Please ensure that all queries are answered when returning your proof corrections so that publication of your article is not delayed.

<b>Query reference</b>	<b>Query</b>	<b>Remarks</b>
Q1	For your information: You can cite this article before you receive notification of the page numbers by using the following format: (authors), J. Mater. Chem. B, (year), DOI: 10.1039/c6tb02150f.	
Q2	Please carefully check the spelling of all author names. This is important for the correct indexing and future citation of your article. No late corrections can be made.	
Q3	Ref. 20, 25 and 58: Can these references be updated?	
Q4	Ref. 38: Please provide details of the last page number for this article.	

Microfluidic generation of alginate microgels for  
the controlled delivery of lentivectors†Justin L. Madrigal,<sup>a</sup> Roberta S. Stilhano,<sup>a</sup> Christian Siltanen,<sup>a</sup> Kimberly Tanaka,<sup>a</sup>  
Sabah Rezvani,<sup>a</sup> Ryan Morgan,<sup>a</sup> Alexander Revzin,<sup>a</sup> Sang W. Han<sup>b</sup> and  
Eduardo A. Silva\*<sup>a</sup>

Cite this: DOI: 10.1039/c6tb02150f

Lentivectors are widely used for gene delivery and have been increasingly tested in clinical trials. However, achieving safe, localized, and sufficient gene expression remain key challenges for effective lentivectoral therapy. Localized and efficient gene expression can be promoted by developing material systems to deliver lentivectors. Here, we address the utility of microgel encapsulation as a strategy for the controlled release of lentivectors. Three distinct routes for ionotropic gelation of alginate were incorporated into microfluidic templating to create lentivector-loaded microgels. Comparisons of the three microgels revealed marked differences in mechanical properties, crosslinking environment, and ultimately lentivector release and functional gene expression *in vitro*. Gelation with chelated calcium demonstrated low utility for gene delivery due to a loss of lentivector function with acidic gelation conditions. Both calcium carbonate gelation, and calcium chloride gelation, preserved lentivector function with a more sustained transduction and gene expression over 4 days observed with calcium chloride gelled microgels. The validation of these two strategies for lentivector microencapsulation may provide a platform for controlled gene delivery.

Received 22nd August 2016,  
Accepted 11th October 2016

DOI: 10.1039/c6tb02150f

www.rsc.org/MaterialsB

## Introduction

Gene therapy has been envisioned to treat a wide range of diseases and disorders.<sup>1</sup> Viral-based strategies, in particular, predominate therapeutic usage due to their higher efficiency of gene expression relative to their non-viral counterparts.<sup>2,3</sup> Lentivectors pseudotyped with VSV-g protein are extensively used because of wide tropism, infectivity for both dividing and non-dividing cells, and low immunogenicity.<sup>4–6</sup> Typically, lentivectors are administered either *ex vivo* or *via* bolus injections.<sup>1</sup> However, these routes of administration can provide a challenge to obtaining safe, localized, and sufficient expression.<sup>7</sup> Therefore, there is a need to develop novel delivery systems that guide the timing, dosage, and localization of lentivectors, which may improve the safety and efficiency by minimizing off-target expression and regulating vector concentrations in target tissue.<sup>2,8–10</sup>

Biomaterial systems could be designed to locally present lentivectors in a sustained manner. More specifically, hydrogels

are an especially attractive class of biomaterials for controlled delivery strategies due to their high-water content, ease of administration, and chemical and structural versatility.<sup>11–15</sup> These hydrogels can be designed to provide a localized depot of lentivectors that can be released in a spatio-temporal manner for cellular transduction.<sup>11,14</sup> Recently, the advent of droplet microfluidic technologies has allowed for the formation of hydrogels in discrete volumes with characteristic dimensions on the order of micrometers.<sup>16</sup> These microgels are generated through emulsion templating, where precursor polymers are emulsified through a flow focusing junction prior to gelation, leading to controllable and monodisperse size.<sup>17,18</sup> In contrast to macroscopic hydrogels, microgels exhibit reduced characteristic lengths and increased surface area, which provides potential for manipulation as a delivery platform. These strategies have been used to promote cellular encapsulation,<sup>19,20</sup> control drug release,<sup>21,22</sup> and have formed a platform for responsive materials.<sup>23–26</sup> Microgel encapsulation may hold advantage for the delivery of lentivectors,<sup>27–29</sup> but adapting these microfluidic techniques for producing lentivector-compatible microgels represents an engineering challenge.

Alginate has been widely studied for encapsulation in both macro- and micro-hydrogels because of its inherent biocompatibility and mild crosslinking chemistry with divalent cations.<sup>30</sup> Recent work demonstrated the capability of degradable alginate hydrogels to deliver lentivectors to the murine hindlimb.<sup>14</sup>

<sup>a</sup> Department of Biomedical Engineering, University of California, 1 Shields Ave., Davis, CA, 95616, USA. E-mail: estilva@ucdavis.edu; Fax: +1-530-754-5739; Tel: +1-530-754-7107

<sup>b</sup> Department of Biophysics, Federal University of São Paulo, São Paulo, Brazil

† Electronic supplementary information (ESI) available. See DOI: 10.1039/c6tb02150f

1 Alginate-delivered lentivectors led to a prolonged gene expres- 1  
sion in comparison to a bolus injection, but there was an initial 2  
delay in expression which can be connected with a slow 3  
lentivector release. The release kinetics could be modified by 4  
altering alginate microgels fabrication methods, but suitable 5  
microfluidic strategies for encapsulating lentivectors remain to 6  
be identified.<sup>31</sup> While early work produced alginate microgels 7  
through the extrusion of alginate droplets into crosslinking 8  
baths,<sup>32–34</sup> recent studies have applied droplet microfluidics 9  
10 to create more monodisperse alginate microgels.<sup>35–39</sup> Several  
strategies for achieving gelation within an emulsion template 11  
have been investigated, including internal and external gelation. 12  
For internal gelation, a sequestered source of divalent cations is 13  
dispersed throughout the alginate solution and released after 14  
15 emulsification. In contrast, external gelation involves infusing  
the carrier phase with a water-soluble divalent cation source 16  
which then partitions into the alginate emulsions. The distinc- 17  
tion between internal and external gelation impacts the cross- 18  
linking time, mechanical structure, and homogeneity of the 19  
20 resulting hydrogel.<sup>40</sup> Importantly, the type of gelation strategy  
applied can decisively affect the cargo biofunctionality after 21  
encapsulation.<sup>37,41</sup> Nevertheless, a side-by-side comparison of 22  
the suitability of these techniques for the encapsulation and 23  
24 release of sensitive therapeutic cargos such as lentivectors has  
not been reported.

To our knowledge, the delivery of lentivectors from alginate 25  
microgels generated with microfluidic templating has not been 26  
evaluated. Here, for the first time we are employing micro- 27  
fluidics to encapsulate lentivectors within alginate microgels in 28  
order to create a controlled delivery system. To identify a 29  
suitable microgel for lentivector delivery, we have directly 30  
compared three microfluidic gelation strategies in terms of 31  
the mechanical properties, encapsulation conditions, and gene 32  
delivery potential. In doing so we have validated two platforms 33  
34 for lentivector delivery from alginate microgels that hold potential  
for improving administration routes for gene therapy.

## 40 Experimental

### 40 Microfluidic device fabrication

Microfluidic devices were fabricated using standard soft litho- 41  
graphy where polydimethylsiloxane (PDMS) elastomer (Sylgard) 42  
was degassed and cured for 1 hour at 70 °C after pouring over 43  
SU-8 master molds prepared on 4-inch silicon wafers (Microchem). 44  
45 Individual PDMS replicas were bonded to glass slides using O<sub>2</sub>  
plasma surface treatment. Finally, microfluidic channels were 46  
made hydrophobic through the application of Aquapel™ solution 47  
for 30 seconds. Flow focusing channel dimensions ( $H \times W$ ) were 48  
49 100 × 100 μm for all droplet generation procedures.<sup>18,20</sup>

### Lentivector

The pCCLc-MNDU3-luciferase-PGK-EGFP-WPRE construct was 50  
kindly obtained from the UC Davis/CIRM Institute for Regenera- 51  
52 tive Cures (Prof. Jan Nolte).<sup>42</sup> The viral titer, which we express  
herein as lentiviral transducing units per mL (TU per mL), was 53  
54

determined as previously reported.<sup>14</sup> Briefly, human embryonic 55  
kidney (HEK-293T) (ATCC) cells were transduced with different 56  
concentrations of lentivectors in the presence of 8 μg mL<sup>-1</sup> of 57  
Polybrene (Sigma). After 3 days, the HEK-293T cells transduced 58  
with lentivector expressing GFP were counted (>10 000 events 59  
60 analyzed) using an Attune flow cytometer (Thermo Fisher) and  
the data was analyzed using FlowJo software (TreeStar Inc.). 61  
Additionally, the viral titer was determined in terms of the 62  
concentration of p24 capsid protein as measured by ELISA 63  
(ZeptoMetrix Co) according to the manufacturer's guidelines 64  
and protocol. A conversion factor of 25 pg per TU was measured 65  
which indicates efficiency in viral packaging.<sup>43,44</sup>

### Generation of alginate microgels

Alginate hydrogels were prepared in three distinct manners at 66  
room temperature to yield micrometer dimension hydrogels, 67  
including (1) internal gelation with calcium carbonate and 68  
glucono delta-lactone (CaCO<sub>3</sub>-GDL),<sup>45</sup> (2) internal gelation 69  
with ethylenediaminetetraacetic acid (EDTA)-chelated calcium 70  
(CaEDTA-AcOH),<sup>41</sup> and (3) external gelation with calcium 71  
chloride (CaCl<sub>2</sub>).<sup>46</sup> All three procedures used a common pre- 72  
cursor polymer solution composed of a binomial mixture of 73  
low and high molecular weight alginates mixed at a 3 : 1 ratio 74  
(LF10/60 and LF20/40, NovaMatrix). Alginate solutions were 75  
prepared fresh for each experiment by dissolving alginates 76  
in 0.9% NaCl overnight at room temperature. For studies 77  
including lentivectors, an appropriate volume of lentivector 78  
suspension was mixed into precursor alginate solutions prior 79  
to droplet formation and gelation. Microgels were imaged 80  
using a Zeiss Axio Vert A.4 phase contrast microscope and 81  
morphology was quantified with Image J.

To prepare CaCO<sub>3</sub>-GDL microgels, an alginate solution 82  
containing suspended CaCO<sub>3</sub> nanoparticles (SkySpring Nano- 83  
materials) and a second alginate solution containing freshly 84  
dissolved GDL (Sigma Aldrich) were mixed on-chip prior to flow 85  
focusing and emulsification.<sup>45</sup> Flow focusing was achieved 86  
using HFE-7500 oil (3 M) with 2% v/v PEGylated fluorosurfactant 87  
(RAN Biotech) as an immiscible carrier phase. The aqueous and 88  
oil flow rates used were 10 μL min<sup>-1</sup> and 50 μL min<sup>-1</sup> respec- 89  
tively. CaCO<sub>3</sub>-GDL microdroplets were collected and incubated 90  
at room temperature for 1 hour to allow for gelation. To collect 91  
the microgels, the droplet emulsion was destabilized using 92  
20% (v/v) perfluorooctanol (Sigma Aldrich) in HFE-7500 and 93  
washed (DMEMc) (Dubelco's Modified Eagle Medium (DMEM) 94  
(Invitrogen) containing 1% penicillin/streptomycin (Invitrogen) 95  
and 10% fetal bovine serum (FBS)(Invitrogen)).

CaEDTA-AcOH microgels were prepared using the same 96  
microfluidic process as stated above but differing in the gela- 97  
tion strategy.<sup>41</sup> Here, chelated calcium was first prepared by 98  
mixing CaCl<sub>2</sub> (Sigma Aldrich) and EDTA (Sigma Aldrich) at equi- 99  
molar ratios at a pH of 7.5. Gelation was initiated immediately 100  
after droplet collection by washing the emulsion with HFE-7500 101  
containing 17.4 mM acetic acid (Sigma Aldrich). Microgels were 102  
then collected from the emulsion as stated above. For both 103  
internal gelation strategies, the ratio between calcium ions and 104  
105 carboxyl moieties on the alginate backbone was kept constant

at 0.36. For CaCO<sub>3</sub>–GDL gelation a constant ratio between CaCO<sub>3</sub> and GDL of 0.5 was maintained for pH balance.

CaCl<sub>2</sub> microgels were prepared using a second microfluidic chip design (Fig. 1) that includes a second inlet for a calcium infused carrier phase. CaCl<sub>2</sub> infused mineral oil was prepared by sonication of a 1 : 9 volumetric mixture of 0.7 g mL<sup>-1</sup> CaCl<sub>2</sub> and light mineral oil (Sigma Aldrich) with 1.2% SPAN 80 (Sigma Aldrich). Here, flow focusing was achieved using light mineral oil with 1.2% SPAN 80 as an immiscible carrier phase. Downstream, CaCl<sub>2</sub> infused mineral oil was used to replace the carrier phase. Flow rates were 2, 6, and 15 μL min<sup>-1</sup> for the aqueous, mineral oil, and calcium infused mineral oil, respectively. The microgels were then collected by centrifugation at (10 rcf) for 3 minutes.

### Rheologic characterization of microgels

Measurements of storage and loss shear moduli were performed using a Discovery HR2 hybrid rheometer (TA instruments) with an 8 mm parallel-plate geometry in time sweep and strain sweep modes.<sup>47</sup> Pre-hydrogel solutions were mixed and crosslinked within the parallel plate geometry. The linear viscoelastic region was determined *via* strain sweep analysis of fully crosslinked hydrogels. Time sweeps were then performed within the linear viscoelastic regime at a strain of 0.3%, and a frequency of 1 rad s<sup>-1</sup>, and a temperature of 23 °C to monitor the development of hydrogel crosslinking. Gelation crossover time was measured as the point where tan(δ) = 1. Geometry edges were coated with sunflower seed oil to prevent evaporation during measurement.

### Equilibrium swelling behavior of microgels

Microgels were prepared and incubated on top of cell strainers (30 μm mesh size, BD) in phosphate buffered saline supplemented with 0.1 g L<sup>-1</sup> CaCl<sub>2</sub> and 0.1 g L<sup>-1</sup> MgCl<sub>2</sub> (PBS<sup>++</sup>) (Invitrogen) at 37 °C for 24 hours. The excess PBS<sup>++</sup> was strained and thoroughly blotted from around the microgels and the wet weight of the microgels was measured. Microgels were then frozen at -20 °C for 24 hours and lyophilized for an additional 24 hours at which point the dry weights of the microgels were measured. The degree of swelling, *Q*, was defined as the reciprocal of the polymer volume fraction in the hydrogel (*v*<sub>2</sub>):

$$v_2 = \frac{1}{\rho_P} \left( \frac{Q_m}{\rho_w} + \frac{1}{\rho_P} \right)^{-1} \quad (1)$$

$$Q = v_2^{-1} \quad (2)$$

Here,  $\rho_P$  is the density of alginate (1.515 g cm<sup>-3</sup>),  $\rho_w$  is the density of water, and  $Q_m$  is the swelling ratio of wet mass over dry mass for the microgels.<sup>48</sup>

### Mesh size calculation

Mesh size for the hydrogels was estimated using swelling and rheometry data.<sup>49–51</sup> The molecular weight between crosslinks ( $M_c$ ) was calculated from the shear modulus elastic component ( $G'$ , Pa) using the following equation:

$$M_c = C_p RT / G' \quad (3)$$

where  $C_p$  is the concentration of alginate,  $R$  is the gas constant, and  $T$  is the temperature at which the measurement was taken. From here, a characteristic mesh size ( $\xi$ ) was calculated as follows:

$$\xi = v_2^{-1/3} l \left( 2 \frac{M_c}{M_r} \right)^{1/2} C_n^{1/2} \quad (4)$$

where  $M_r$  is the molecular weight of the repeating unit (194 g mol<sup>-1</sup>),  $l$  is the length of the repeating unit (5.15 Å) and  $C_n$  is the characteristic ratio  $C_n = 0.021 M_n + 17.95 = 21.1$ .<sup>52</sup>

### Monitoring of pH during microgel gelation

A pH probe (Mettler Toledo) was immersed within alginate solutions and gelation was initiated to form a hydrogel around the probe. pH measurements were recorded once per minute for three hours ( $n = 2$ ). Additionally, hydrogels were prepared in the same manner and the pH was measured after one hour ( $n = 3$ ).

### Effect of pH and encapsulation on lentivector functionality

Lentivector suspensions were pre-incubated in media with adjusted pH values. For pH treatment, media was equilibrated with acetic acid to pH levels of 5.0, 6.0, 6.5, and 7.5. Lentivector suspension containing  $6 \times 10^4$  TU were incubated within treated media, and following times of 10, 30, and 60 minutes, the lentivector suspension was diluted with DMEMc and applied to HEK-293T cells. Alternatively,  $7.5 \times 10^4$  TU of lentivectors were encapsulated within alginate microgels, released by hydrogel enzymatic digestion with alginate lyase<sup>53</sup> (Sigma Aldrich), and then applied to HEK-293T cells. For all experiments the transduction efficiency of the lentivectors was quantified by flow cytometry (> 10 000 events analyzed).

### Quantification of lentivector release from alginate microgels

Alginate microgels (1% alginate) were prepared using the CaCl<sub>2</sub> and CaCO<sub>3</sub>–GDL procedures described above and loaded with 8250 TU per μL. 12 μL of microgels were collected and immersed within DMEMc in microcentrifuge tubes at 37 °C and 5% CO<sub>2</sub> to allow for lentivector release ( $n = 2–3$ ). At selected time points spanning 10 days, the supernatant was collected and stored at -20 °C (until sample concentration was determined), and a fresh aliquot of medium was added over each disk. Alternatively, lentivectors were immediately recovered from a separate 12 μL of microgels by digestion with 10 units per mL of alginate lyase<sup>53</sup> ( $n = 3$ ). The concentrations of lentivectors in supernatant and digestion samples were determined in terms of the p24 capsid protein. The p24 concentrations were quantified using an HIV p24 Antigen ELISA Kit (ZeptoMetrix Co) according to the manufacturer's guidelines and protocol as has previously described.<sup>14,54</sup>

### Transduction efficiency of lentivector-loaded alginate microgels

In all the experiments detailed below,  $3 \times 10^4$  HEK-293T cells were seeded per well in 24-well plates and cultured in DMEMc for 24 hours at 37 °C and 5% CO<sub>2</sub> prior to any contact with lentivectors. Alginate microgels (1% alginate) were prepared

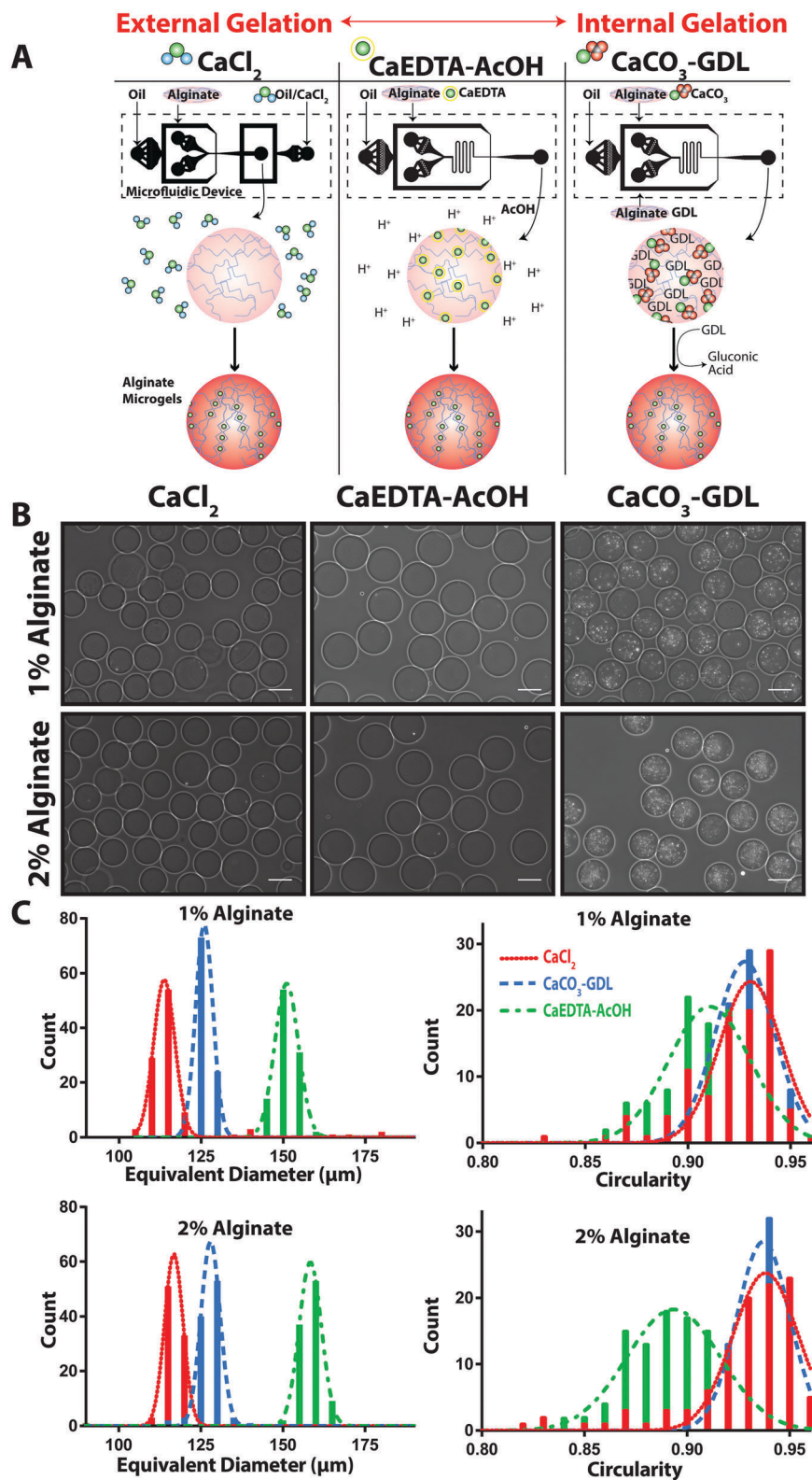


**Fig. 1** Morphological characterization of alginate microgels. Illustration of the formulation of three distinct microgels fabricated from microfluidics devices (A). Representative phase-contrast photomicrographs of alginate microgels fabricated using three different gelation techniques (B). Microgels with controlled dispersity in microgel diameter (C) and circularity (D) were obtained by use of microfluidic templating ( $n = 103$  microgels). Calibration bar represents  $100 \mu\text{m}$ .

55 using the  $\text{CaCl}_2$  and  $\text{CaCO}_3\text{-GDL}$  procedures as described above and loaded with  $8250 \text{ TU per } \mu\text{L}$  of lentivectors.  $12 \mu\text{L}$  of microgels (total  $\text{MOI} = 3.5$ ) were suspended in  $250 \mu\text{L}$  DMEMc. The medium of HEK-293T was then replaced with

1 the microgel suspension. After 12 hours, an additional 750  $\mu\text{L}$  of DMEMc was added to each well and incubated for an additional 12 hours. Following this first day, the media containing the microgel suspension was collected and replaced with  
 5 DMEMc and the cells were cultured for an additional 24 hours to allow for GFP expression. The microgels were then recovered from the collected media by centrifugation (30 rcf) for 3 minutes and were resuspended in 250  $\mu\text{L}$  of fresh DMEMc. This microgel suspension was then added to HEK-293T cells which had been  
 10 seeded the prior day and the cycle was repeated for a total of 4 days. The transduced HEK-293T cells from each time point were incubated for 48 hours for determination of transduction efficiency as previously described.<sup>55,56</sup> In the negative control wells only DMEMc was added, and in the positive control wells  
 15 DMEMc with lentivector ( $3 \times 10^5$  TU per well) was added. The transduction efficiency was assessed both qualitatively and quantitatively *via* fluorescent microscopy (Axio Vert.A1; Zeiss) and flow cytometry counting GFP-positive cells ( $> 10\,000$  events analyzed/experimental condition).

### 20 Statistical analysis

All statistical analyses were performed using Student *t*-tests (two-tail comparisons) or one-way analysis of variance (ANOVA) with *post hoc* Tukey's test unless stated otherwise, and analyzed  
 25 using Prism 6 software (Graphpad). Differences between conditions were considered significant if  $P < 0.05$ .

## 30 Results

### 30 Characterization microgel dimensions and morphology

In this study, we investigated the utility of microfluidic strategies for the encapsulation of lentivectors within alginate microgels. Three distinct gelation mechanisms were tested including two strategies employing internal gelation and one using an external gelation approach (Fig. 1A). One internal gelation strategy used calcium carbonate, which releases  $\text{Ca}^{2+}$  upon the slow hydrolysis and acidification of GDL ( $\text{CaCO}_3\text{-GDL}$ ).<sup>40</sup> Here, a stoichiometric ratio of  $\text{CaCO}_3$  to GDL is maintained in order to minimize the acidification of the crosslinking environment. Furthermore, the crosslinking proceeds in a gradual and controlled manner. The other internal gelation strategy takes advantage of the preferential affinity of EDTA for divalent cations at basic pH (CaEDTA-AcOH).<sup>41</sup> Here, chelated  $\text{Ca}^{2+}$  is loaded into alginate and released by an abrupt drop in pH. The resultant crosslinking is rapid, which minimizes the duration of, but does not avoid, potentially harmful acidic gelation conditions. Distinctively, the external gelation approach infused the carrier oil with calcium chloride and allowed partitioning into the aqueous alginate

1 phase to initiate gelation.<sup>45</sup> Again, the crosslinking is rapid, but no associated drop in pH is to be expected. Importantly, all three strategies yielded microgels with approximately spherical morphology and micrometer equivalent diameters (Fig. 1B, C and Table 1). Microgels fabricated using either the calcium  
 5 chloride bath or EDTA caged calcium produced transparent hydrogels in comparison to the calcium carbonate method. Calcium carbonate precipitate remains visible after 1 hour of gelation. With extended gelation times these microgels became transparent indicating that for full calcium dissolution length-  
 10 ened times may be necessary.

### Mechanical testing of hydrogels

To analyze the mechanical properties of hydrogels generated by the three gelation strategies, both macroscopic hydrogel disks and microgels were fabricated for testing. Rheological testing identified the time at which the storage modulus surpassed the loss modulus, and provided the maximum storage modulus of macroscopic disks (Fig. 2). For CaEDTA-AcOH and  $\text{CaCl}_2$  hydrogels, respective plateaus in storage modulus of  $2.3 \pm 0.7$  kPa (2% alginate),  $0.5 \pm 0.2$  kPa (1% alginate) and  $9.5 \pm 1.3$  kPa (1% alginate) and  $35.3 \pm 9.3$  kPa (2% alginate) were reached within the first minute after the addition of either acetic acid or  $\text{CaCl}_2$  respectively. In comparison, 2.5 minutes passed for gelation and more than 30 minutes was required to reach a plateau in storage modulus for the slow  $\text{Ca}^{2+}$   
 25 releasing  $\text{CaCO}_3\text{-GDL}$  method (Table 1 and Fig. 2A). The final storage modulus of  $\text{CaCO}_3\text{-GDL}$  gels plateaued at values of  $4.0 \pm 0.6$  kPa (1%) and  $18.7 \pm 3.5$  kPa (2%). For all three formulations, there was an increase in storage modulus when alginate concentration increased from 1 to 2% (Fig. 2B). While gelation kinetics are expected to differ between microgel and macro-scale disks, our rheological data correlated closely with swelling behavior observed in microgels. Here, CaEDTA-AcOH microgels exhibited greater swelling ratios,  $57.1 \pm 2.2$  (1% alginate) and  $40.7 \pm 5.9$  (2% alginate), than  $\text{CaCl}_2$  microgels,  $40.5 \pm 6.6$  (1% alginate) and  $24.1 \pm 1.8$  (2% alginate), and  $\text{CaCO}_3\text{-GDL}$  microgels,  $29.5 \pm 1.3$  (1% alginate) and  $24.8 \pm 1.6$  (2% alginate) with a similar dependence on polymer content as was seen with storage modulus (Fig. 2C). In addition, the mesh size was calculated from the measured storage modulus and swelling data and yielded values of  $18 \pm 5$  nm and  $9.9 \pm 2$  nm for 1% and 2% CaEDTA-AcOH microgels,  $4.8 \pm 0.4$  nm and  $2.9 \pm 0.3$  nm for 1% and 2%  $\text{CaCO}_3\text{-GDL}$  microgels, and  $3.4 \pm 0.3$  nm and  $2.1 \pm 0.3$  nm for 1 and 2%  $\text{CaCl}_2$  microgels (Fig. 2D).

### Particle encapsulation efficiency

To determine the ability to encapsulate and recover cargo, microgels were loaded with fluorescently labeled polystyrene

50 **Table 1** Summary of microgel production and morphological characterization

Microgel	Production rate ( $\mu\text{L min}^{-1}$ )	Ca:COOH	Crossover time (seconds)		Equivalent diameter ( $\mu\text{m}$ )		Circularity	
			1%	2%	1%	2%	1%	2%
$\text{CaCl}_2$	2	NA	$< 5$	$< 5$	$104 \pm 8.4$	$98.5 \pm 16$	$0.91 \pm 0.045$	$0.91 \pm 0.049$
CaEDTA-AcOH	10	0.36	$< 5$	$< 5$	$152 \pm 13$	$159 \pm 11$	$0.91 \pm 0.020$	$0.90 \pm 0.021$
$\text{CaCO}_3\text{-GDL}$	10	0.36	$153 \pm 21$	$138 \pm 43$	$126 \pm 2.5$	$127 \pm 5.0$	$0.92 \pm 0.017$	$0.93 \pm 0.018$

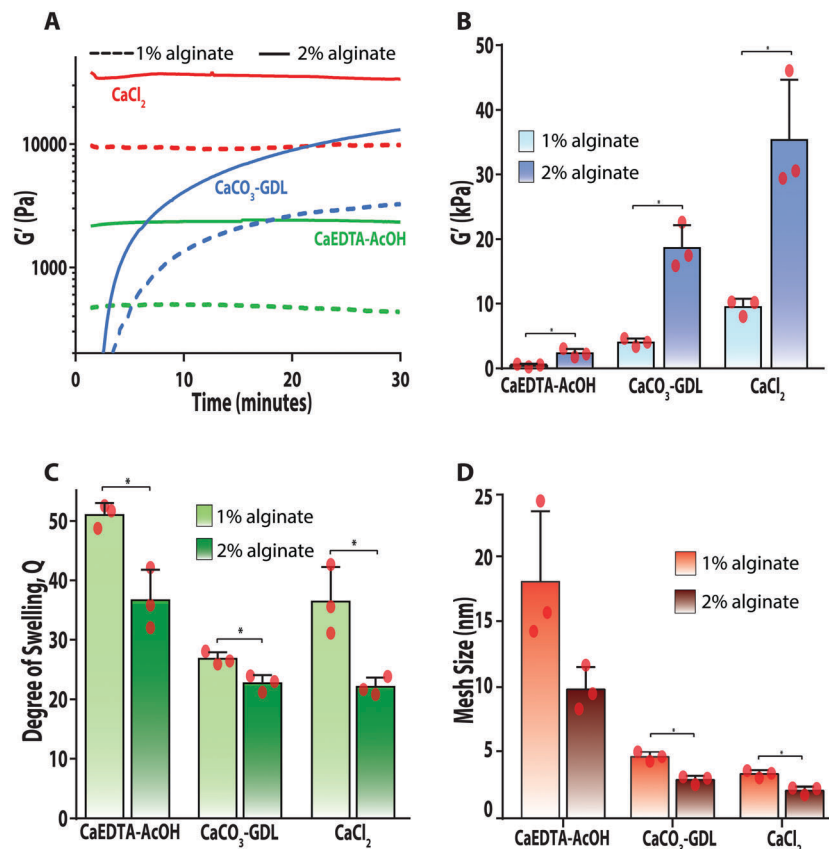


**Fig. 2** Structural characterization of alginate hydrogels. Alginate hydrogels gelled via  $\text{CaCO}_3\text{-GDL}$  display an evolution of storage modulus in comparison to hydrogels gelled via either  $\text{CaCl}_2$  or  $\text{CaEDTA-AcOH}$  (A). The plateau storage modulus of hydrogels (B) and equilibrium swelling behavior of microgels (C) incubated at  $37^\circ\text{C}$  in PBS indicate increased crosslinking with the use of  $\text{CaCl}_2$  or  $\text{CaCO}_3\text{-GDL}$ . Mesh sizes of hydrogels calculated from collected swelling and rheological data (D). \* indicates statistically significant differences ( $P < 0.05$ ). Bar represent mean, scatter dot plots displays individual measurements and error bars represents standard deviation. (A–D,  $n = 3$ ).

particles with diameters on the same order of magnitude as lentivectors (100 nm). The encapsulation was visualized by the localized fluorescence within microgels and all three formulations demonstrated a near full recovery ( $>90\%$ ) of the loaded particles after enzymatic digestion of the microgels (Fig. S1, ESI†).

#### Effect of pH and encapsulation on lentivector functionality

We measured pH levels during gelation of macroscopic hydrogels by each of the three strategies (Fig. 3A). The pH remained constant during the  $\text{CaCl}_2$  gelation strategy. For  $\text{CaCO}_3\text{-GDL}$ , pH decreased slowly from 7 to 5.8 over the course of three hours. In practice, we found these microgels were sufficiently crosslinked after only one hour (pH 6.3), at which point they are washed into buffered media (Fig. 3B). In contrast,  $\text{CaEDTA-AcOH}$  resulted in an abrupt drop in pH to 4.3, but only 5 minutes is required before washing into buffered media.

Subsequently, to assess lentivector sensitivity to pH we studied the capability of lentivectors to transduce HEK-293T after exposure to acidified media (Fig. 3C). Lentivectors pre-incubated with acidified media had a diminished ability to transduce HEK-293T cells. This harmful effect was exaggerated as the duration of pre-incubation was lengthened and was statistically significant compared to neutral media for all pH

tested after one hour of pre-incubation. At a pre-incubation pH of 6.5 no effect was observed for the first 30 minutes, however at 1 hour a marginal drop to  $89 \pm 3.2\%$  of the control transduction efficiency occurred. At a pH of 6.0 a drop to  $91 \pm 1.0\%$  and then  $82 \pm 1.4\%$  was observed after 30 minutes and 1 hour respectively. For a pH of 5.0 the transduction efficiency dropped to  $78 \pm 0.6\%$  after 30 minutes and was reduced to  $73 \pm 1.7\%$  after 1 hour.

Next, lentivectors were encapsulated within the different microgels and the viability of the lentivectors was tested (Fig. 3D). Immediately following encapsulation, lentivectors were released by enzymatic digestion of the microgels and the functionality of the released lentivectors was analyzed. No significant reduction in transduction efficiency was observed after encapsulation in either  $\text{CaCl}_2$  or  $\text{CaCO}_3\text{-GDL}$  microgels. However, for  $\text{CaEDTA-AcOH}$  a dramatic drop in transduction efficiency to  $4.3 \pm 0.5\%$  of the control was observed. Accordingly,  $\text{CaEDTA-AcOH}$  microgels were not considered in the following studies.

#### Loading and release of lentivectors from microgels

We next studied the encapsulation efficiency and release profile for lentivectors encapsulated within  $\text{CaCO}_3\text{-GDL}$  and  $\text{CaCl}_2$

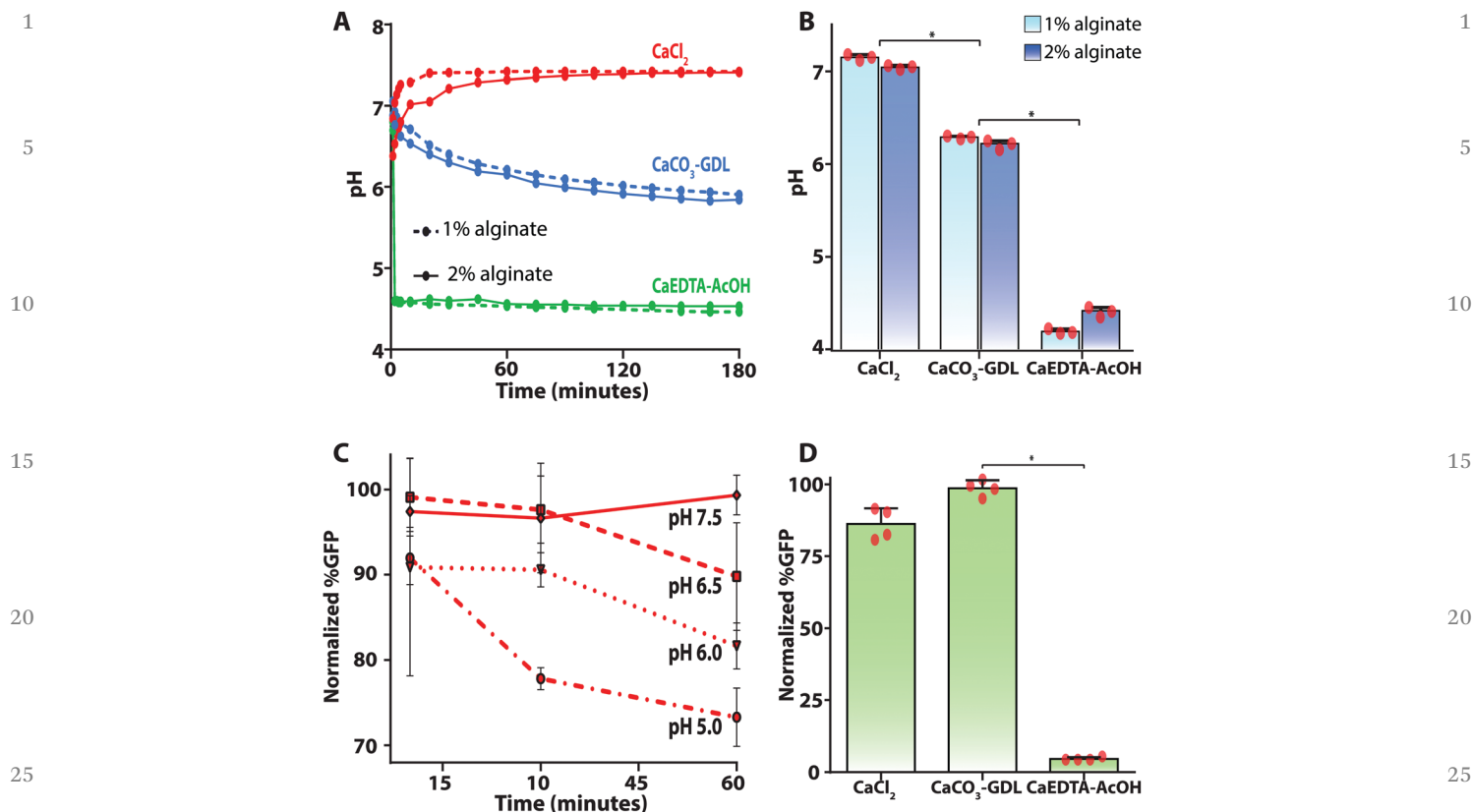


**Fig. 3** Lentivector sensitivity to hydrogel gelation environment. The pH profile during hydrogel gelation was monitored in macroscopic gels (A) and the pH after 1 hour demonstrates a minimal pH drop for CaCO<sub>3</sub>-GDL hydrogels (B). Lentivectors demonstrated a loss of function after pre-incubation for increasing amounts of time in acidified media prior to transduction of HEK-293T cells (C). Lentivectors were encapsulated within alginate microgels and immediately released *via* hydrogel digestion and the transduction potential of the lentivector was analyzed *via* flow cytometry (D). \* indicates statistically significant differences ( $P < 0.005$ ). Bar represent mean, scatter dot plots displays individual measurements and error bars represent standard deviation. (A,  $n = 2$ ; B,  $n = 3$ ; C and D,  $n = 4$ ).

microgels (1% alginate). For both formulations, the total amount of p24 capsid protein recovered from digested microgels was close to the initial amount loaded with encapsulation efficiencies of  $1.3 \pm 0.4$  and  $1.1 \pm 0.1$  for the CaCO<sub>3</sub>-GDL and CaCl<sub>2</sub> microgels respectively (Fig. 4A). In parallel to the encapsulation efficiency, the release of lentivectors was measured over the course of 10 days (Fig. 4B). Here, a more gradual release was observed for the CaCl<sub>2</sub> microgels compared with a faster initial release observed with the CaCO<sub>3</sub>-GDL microgels. After 6 hours, 7.3% of the encapsulated p24 capsid protein was released from CaCl<sub>2</sub> microgels compared with 36.1% released from the CaCO<sub>3</sub>-GDL microgels. However, following this initial burst, the release from CaCO<sub>3</sub>-GDL microgels plateaued. Consequently, over the course of 10 days, both formulations had released approximately 60% of the loaded lentivectors.

#### Lentivector transduction from alginate microgels

Finally, we evaluated the potential and efficiency of the alginate microgels to serve as a controlled release system for lentivectors that retain their transduction activity over time (Fig. 5). Lentivector-loaded microgels were suspended above HEK-293T cell monolayers over the course of four days. A new monolayer of cells was exposed to the lentivector-loaded microgels every 24 hours.

As a positive control, lentivectors in suspension were used and demonstrated efficient transduction (95%). Successful GFP expression was observed in cells brought into contact with both the CaCO<sub>3</sub>-GDL and CaCl<sub>2</sub> microgels. The gene expression as assessed *via* fluorescence microscopy (Fig. 5A) demonstrates the preservation of lentivector function and ability to escape from the microgel meshwork. In parallel, quantification of GFP expression *via* flow cytometry revealed a difference in the relative profiles of transduction brought about by the two formulations (Fig. 5B). For both formulations, transduction efficiency was highest during the first 24 hours of lentivector release. However, this initial burst release was greater for CaCO<sub>3</sub>-GDL microgels. For cells exposed to the first 24 hours of lentivector release there was significantly higher transduction from the CaCO<sub>3</sub>-GDL microgels (51%) compared with the CaCl<sub>2</sub> microgels (18.9%). Following this high level of transduction, the percentage of cells transduced by the CaCO<sub>3</sub>-GDL microgels dropped to 33% and then 4.8% for cells in contact with microgels during release times of 24–48 hours and 48–72 hours respectively. Little transduction was observed on subsequent days (<1%). In comparison, the CaCl<sub>2</sub> microgels sustained a more consistent level of transduction with 7.1% at 24–48 hours, 10.3% at 48–72 hours, 5.9% at 72–96 hours, and 6.7% at 96–120 hours.

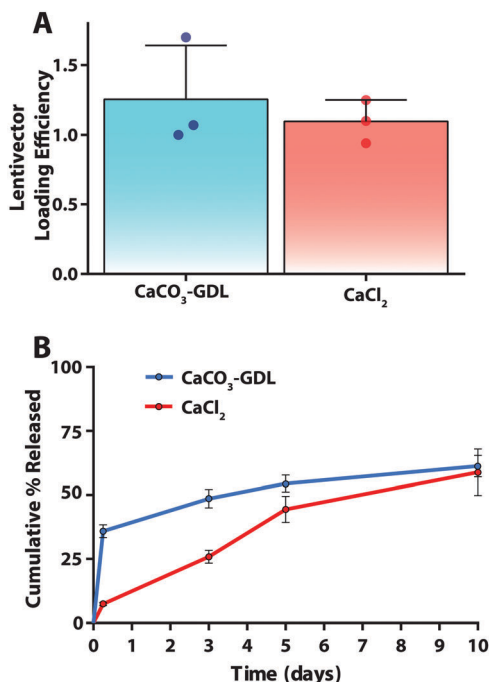


Fig. 4 Lentivector encapsulation efficiency and release profiles. Efficient loading of lentivectors within microgels was measured for microgel formulations (A). The release profile of encapsulated lentivectors was evaluated in terms of p24 capsid protein over the course of ten days indicating a more controlled release with the CaCl<sub>2</sub> microgels (B). On A, bar represent mean, scatter dot plots display individual measurements and error bars represent standard deviation. (A,  $n = 3$ ; B,  $n = 2-3$ ).

## Discussion

The results of this study demonstrate the capability of alginate microgels, fabricated using microfluidic technology, to successfully encapsulate and release functional lentivectors for gene delivery *in vitro*. Three alginate gelation strategies were successfully combined with microfluidic templating to generate microgels. While these procedures yielded monodisperse, spherical structures with high loading efficiencies, discernable differences between the three in overall mechanical properties, lentivector release, and cellular transduction were observed. Together, these results highlight microgel crosslinking and pH control as key variables for efficient delivery of lentivectors, and identify two potential platforms for an alginate-microgel lentivector delivery system.

The main objective of this work was to identify suitable strategies for encapsulating lentivectors in alginate microgels for controlled release and cellular transduction. We have adapted three microfluidic gelation strategies towards this goal.<sup>41,45,46</sup> Alginate is emulsified into droplet templates and crosslinked using either internal or external ionotropic gelation which yields, for all three strategies, microgels with tight control over size and morphology. While successfully generating microgels, the three gelation strategies are distinct in the mechanical properties they impart on the final hydrogel, which will in turn affect the expected release profiles of encapsulated cargo. The diameter of the microgels varied slightly between

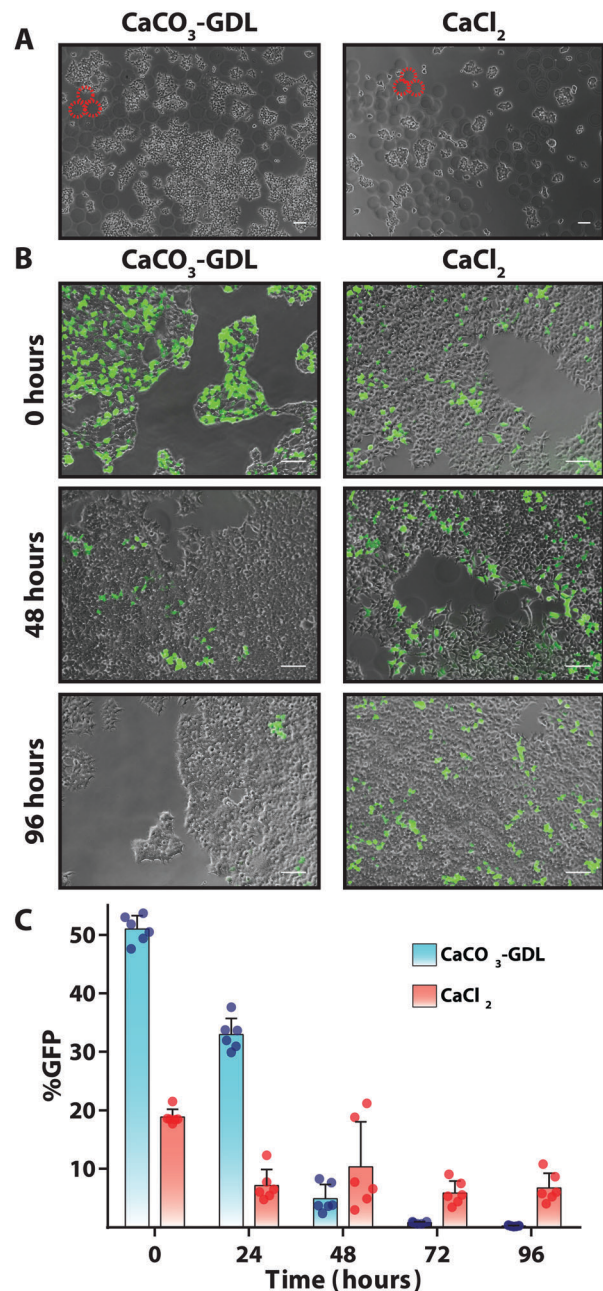


Fig. 5 *In vitro* transduction over time via lentivectors released from alginate microgels. Phase-contrast images of lentivectors-loaded microgels in contact with HEK-293T cells with three representative microgels outlined in red-dashed line (A). Representative merged phase-contrast/fluorescent photomicrographs of HEK-293T cell monolayers after exposure to lentivector-loaded microgels encoding for GFP at 0, 2 and 4 days after encapsulation (B). Lentivector-loaded microgels were placed in contact with a series of HEK-293T monolayers (contact time 24 hours) and the GFP expression of these cells was then analyzed by flow cytometry (C). Calibration bar represents 100  $\mu\text{m}$ . Bar represent mean, scatter dot plots displays individual measurements and error bars represents standard deviation. (C,  $n = 6$ ).

the three gelation schemes despite flow focusing occurring in all cases through a 100  $\times$  100  $\mu\text{m}$  junction. The final size of the microgels depends on the size of the emulsion template and

1 the degree of crosslinking. In practice, the size of the emulsions  
can be tuned by altering the relative flow rates of the oil and  
aqueous phases or changing the size of the flow focusing  
junction (data not shown). External gelation produced the  
smallest diameter microgels, highest storage moduli, and low-  
est degree of swelling. In macroscopic systems, and likely here  
in the microfluidic system, external gelation creates a gradient  
of polymer and crosslinking concentration and makes control  
over total calcium content and gelation rates difficult to  
achieve.<sup>40,57,58</sup> In comparison, internal gelation allows for a  
consistent calcium to carboxyl molar ratio to be set.<sup>40</sup> The  
resulting microgels exhibited larger diameters, diminished  
storage moduli, and higher degrees of swelling in comparison  
to external gelation. Specifically, these differences were signifi-  
cantly pronounced for CaEDTA-AcOH in comparison to  
CaCO<sub>3</sub>-GDL. This discrepancy may be due to gelation kinetics  
and the extent to which the sequestered calcium is fully  
released. Alginate crosslinked at slower rates produces hydro-  
gels of increased mechanical integrity which has been attrib-  
uted to an increased order of the network structure.<sup>31,40,59</sup>  
CaCO<sub>3</sub>-GDL hydrogels undergo gradual crosslinking, as was  
evident here by the evolution of the storage modulus over time,  
due to the gradual hydrolysis of GDL to gluconic acid and  
concomitant gradual release of calcium from the carbonate  
salt.<sup>40,45,60</sup> In comparison, CaEDTA-AcOH gelation occurred  
rapidly alongside a drop in pH, and it is possible that the  
reversible nature of calcium-EDTA interactions may inhibit  
gelation to some extent.

In addition to differences in mechanical properties the three  
gelation strategies impart different encapsulation environments.  
These environmental conditions (temperature, pH, ionic strength,  
shear stress, *etc.*) to which lentivectors will be exposed can  
dramatically affect stability and infectivity.<sup>61</sup> Previous studies have  
shown a severe reduction in the half-life of VSV-G pseudotyped  
retroviral vectors at a pH of 6.<sup>62</sup> Similarly, ecotropic moloney  
murine leukemia virus has a narrow window of infectivity between  
a pH of 5.5 and 8.0 with irreversible damage outside of this  
range.<sup>63</sup> Here, the need for acid-mediated cation release for both  
internal gelation strategies becomes an important consideration  
for developing a viable encapsulation strategy. While both internal  
gelation strategies require an acid, the pH of the CaCO<sub>3</sub>-GDL is  
controlled by setting a stoichiometric ratio of GDL to CaCO<sub>3</sub>. The  
pH drop is minimal as GDL is hydrolyzed to gluconic acid and  
then further neutralized by reaction with calcium carbonate.  
Conversely, dissociation of calcium-EDTA complexes is depen-  
dent upon a sharp drop in pH.<sup>64</sup> A marked loss of transduction  
efficiency was observed for lentivectors encapsulated within  
CaEDTA-AcOH microgels, and accordingly this system was  
removed from further consideration as a viable lentivector delivery  
system for this study.

The control of lentivirus release can be governed based on  
three key aspects of a hydrogel system: (i) the diffusivity of the  
vector within the hydrogel; (ii) the degradability of the hydrogel;  
and (iii) the affinity between the polymers used and the  
vector.<sup>11</sup> However, the exact mechanism for lentivector release  
from alginate hydrogels remains to be elucidated. Diffusion of

lentivectors through an alginate meshwork will be severely  
diminished due to the relative size of lentivectors ( $\sim 100$  nm)<sup>65</sup>  
and alginate mesh size ( $\sim 10$  nm).<sup>66-68</sup> Nevertheless, we have  
observed release of lentivectors from both macroscopic alginate  
hydrogels<sup>14</sup> and microgels. For microgels it is possible that  
increased surface area contributes to the amount of lentivectors  
released. Additionally, the reported mesh sizes may not com-  
pletely prevent the transport of such particles through the  
mesh.<sup>54,69,70</sup> This measurement provides only an approximation  
of an idealized meshwork structure, and in reality does not  
account for network imperfections such as closed polymer loops,  
dangling ends, and slipping chain entanglements.<sup>71</sup>

Interestingly, the profiles of lentivector release and cellular  
transduction suggest that the mode of gelation and extent of  
crosslinking may be important parameters in regulating lentivec-  
tor delivery from microgels. While a large burst release was  
observed for CaCO<sub>3</sub>-GDL microgels, a more gradual and sustained  
release was achieved using CaCl<sub>2</sub> microgels. The calculation of  
mesh sizes revealed a more compact network for the tightly  
crosslinked CaCl<sub>2</sub> microgels. In addition to a tighter network,  
the gradient crosslinking that occurs with external gelation has  
been correlated to decreased surface permeability.<sup>72</sup> Together,  
these phenomena may explain the slower release and sustained  
transduction that was observed with CaCl<sub>2</sub> microgels, but further  
studies within one gelation strategy will be needed to elucidate the  
role that these parameters play in lentivector release. Encoura-  
gingly, these studies provide a foundation for creating microgels  
with different kinetics of lentivector release. As such, future studies  
can aim to generate systems where multiple patterns of lentivector  
delivery can be incorporated into a single mixture of microgels.

## Conclusions

In summary, we have for the first time investigated microfluidic  
templating as a strategy to encapsulate lentivectors within alginate  
microgels. We directly compared three processes and have  
identified that internal gelation with CaCO<sub>3</sub>-GDL and external  
gelation with CaCl<sub>2</sub> are suitable for creating lentivector compa-  
tible microgels. The profiles of lentivector release from these  
microgels correlated with measured mechanical properties and  
suggest that the overall crosslinking density and homogeneity of  
alginate microgels can be used as tunable parameters to adjust  
the release of lentivectors. This strategy can be advantageous for  
the controlled delivery multiple vectors as it becomes possible to  
engineer suites of microgels with desired release rates. Given the  
flexibility of genes that can be transduced with lentivectors, the  
engineering of such delivery systems may provide benefit across  
a wide range of therapeutic applications.

## Sources of funding

Financial support of this research was provided by the University of  
California, Davis, American Heart Association (15BGIA25730057),  
FAPESP (2015/20206-8) and Hellman Family. RSS was supported by  
a FAPESP scholarship (Grant number: 2012/00753-6). JM was

1 supported by a Howard Hughes Medical Institute (HHMI) Integrating  
 Medicine into Basic Science pre-doctoral fellowship.

## 5 Disclosures

None.

## 10 Acknowledgements

We would like to thank both Prof. Scott Simon's and Prof. Jamal Lewis's (UC Davis) group for all the support and guidance with the flow cytometry experiments. In addition, we would like to thank Prof. Kent Leach's (UC Davis) group for all the support and guidance with rheology experiments. Finally, we want to express our gratitude to Prof. Jan Nolta and Dr Fernando Fierro (UC Davis) for their kind donation of lentivectors.

## 20 References

- 1 L. Naldini, *Nature*, 2015, **526**, 351–360.
- 2 J. H. Jang, D. V. Schaffer and L. D. Shea, *Mol. Ther.*, 2011, **19**, 1407–1415.
- 25 3 S. L. Ginn, I. E. Alexander, M. L. Edelstein, M. R. Abedi and J. Wixon, *J. Gene Med.*, 2013, **15**, 65–77.
- 4 L. Naldini, U. Blomer, P. Gally, D. Ory, R. Mulligan, F. H. Gage, I. M. Verma and D. Trono, *Science*, 1996, **272**, 263–267.
- 30 5 K. Breckpot, J. L. Aerts and K. Thielemans, *Gene Ther.*, 2007, **14**, 847–862.
- 6 J. Matrai, M. K. L. Chuah and T. VandenDriessche, *Mol. Ther.*, 2010, **18**, 477–490.
- 7 M. A. Kotterman, T. W. Chalberg and D. V. Schaffer, *Annu. Rev. Biomed. Eng.*, 2015, **17**, 63–89.
- 35 8 I. C. Liao, S. Chen, J. B. Liu and K. W. Leong, *J. Controlled Release*, 2009, **139**, 48–55.
- 9 Y. F. Zeng, S. J. Tseng, I. M. Kempson, S. F. Peng, W. T. Wu and J. R. Liu, *Biomaterials*, 2012, **33**, 9239–9245.
- 40 10 A. M. Thomas, A. J. Gomez, J. L. Palma, W. T. Yap and L. D. Shea, *Biomaterials*, 2014, **35**, 8687–8693.
- 11 S. K. Seidlits, R. M. Gower, J. A. Shepard and L. D. Shea, *Expert Opin. Drug Delivery*, 2013, **10**, 499–509.
- 12 C. J. Kearney and D. J. Mooney, *Nat. Mater.*, 2013, **12**, 1004–1017.
- 45 13 R. Censi, P. Di Martino, T. Vermonden and W. E. Hennink, *J. Controlled Release*, 2012, **161**, 680–692.
- 14 R. S. Stilhano, J. L. Madrigal, K. Wong, P. A. Williams, P. K. M. Martin, F. S. M. Yamaguchi, V. Y. Samoto, S. W. Han and E. A. Silva, *J. Controlled Release*, 2016, **237**, 42–49.
- 50 15 S. S. McMahon, N. Nikolskaya, S. N. Choileain, N. Hennessy, T. O'Brien, P. M. Strappe, A. Gorelov and Y. Rochev, *J. Gene Med.*, 2011, **13**, 591–601.
- 55 16 B. G. Chung, K. H. Lee, A. Khademhosseini and S. H. Lee, *Lab Chip*, 2012, **12**, 45–59.
- 17 S. Y. Teh, R. Lin, L. H. Hung and A. P. Lee, *Lab Chip*, 2008, **8**, 198–220.
- 18 A. R. Abate, M. Kutsovsky, S. Seiffert, M. Windbergs, L. F. V. Pinto, A. Rotem, A. S. Utada and D. A. Weitz, *Adv. Mater.*, 2011, **23**, 1757–1760.
- 19 R. M. Hernández, G. Orive, A. Murua and J. L. Pedraz, *Adv. Drug Delivery Rev.*, 2010, **62**, 711–730.
- 20 C. Siltanen, M. Yaghoobi, A. Haque, J. You, J. Lowen, M. Soleimani and A. Revzin, *Acta Biomater.*, 2016, DOI: **Q3** 10.1016/j.actbio.2016.01.012. 10
- 21 W.-F. Lai, A. S. Susha and A. L. Rogach, *ACS Appl. Mater. Interfaces*, 2016, **8**, 871–880.
- 22 M. N. Hsu, R. Luo, K. Z. Kwek, Y. C. Por, Y. Zhang and C.-H. Chen, *Biomicrofluidics*, 2015, **9**, 052601.
- 23 J. Wei, X.-J. Ju, X.-Y. Zou, R. Xie, W. Wang, Y.-M. Liu and L.-Y. Chu, *Adv. Funct. Mater.*, 2014, **24**, 3312–3323. 15
- 24 D. R. Griffin, W. M. Weaver, P. O. Scumpia, D. Di Carlo and T. Segura, *Nat. Mater.*, 2015, **14**, 737–744.
- 25 R. Ghaffarian, E. Pérez-Herrero, H. Oh, S. R. Raghavan and S. Muro, *Adv. Funct. Mater.*, 2016, DOI: 10.1002/adfm.201600084. 20
- 26 J.-W. Kim, A. S. Utada, A. Fernández-Nieves, Z. Hu and D. A. Weitz, *Angew. Chem.*, 2007, **119**, 1851–1854.
- 27 S. Kalyanasundaram, S. Feinstein, J. P. Nicholson, K. W. Leong and R. I. Garver, Jr., *Cancer Gene Ther.*, 1999, **6**, 107–112. 25
- 28 H. Park, P.-H. Kim, T. Hwang, O.-J. Kwon, T.-J. Park, S.-W. Choi, C.-O. Yun and J. H. Kim, *Int. J. Pharm.*, 2012, **427**, 417–425.
- 29 G. Sailaja, H. HogenEsch, A. North, J. Hays and S. K. Mittal, *Gene Ther.*, 2002, **9**, 1722–1729. 30
- 30 K. Y. Lee and D. J. Mooney, *Prog. Polym. Sci.*, 2012, **37**, 106–126.
- 31 A. D. Augst, H. J. Kong and D. J. Mooney, *Macromol. Biosci.*, 2006, **6**, 623–633.
- 32 O. Gaserod, A. Sannes and G. Skjak-Braek, *Biomaterials*, 1999, **20**, 773–783. 35
- 33 O. Gaserod, O. Smidsrod and G. Skjak-Braek, *Biomaterials*, 1998, **19**, 1815–1825.
- 34 A. Blandino, M. Macías and D. Cantero, *J. Biosci. Bioeng.*, 1999, **88**, 686–689. 40
- 35 K. S. Huang, T. H. Lai and Y. C. Lin, *Lab Chip*, 2006, **6**, 954–957.
- 36 C. J. Martinez, J. W. Kim, C. Ye, I. Ortiz, A. C. Rowat, M. Marquez and D. Weitz, *Macromol. Biosci.*, 2012, **12**, 946–951. 45
- 37 S. Akbari and T. Pirbodaghi, *Microfluid. Nanofluid.*, 2014, **16**, 773–777.
- 38 W. H. Tan and S. Takeuchi, *Adv. Mater.*, 2007, **19**, 2696–+. **Q4**
- 39 C. H. Choi, J. H. Jung, Y. W. Rhee, D. P. Kim, S. E. Shim and C. S. Lee, *Biomed. Microdevices*, 2007, **9**, 855–862. 50
- 40 C. K. Kuo and P. X. Ma, *Biomaterials*, 2001, **22**, 511–521.
- 41 S. Utech, R. Prodanovic, A. S. Mao, R. Ostafe, D. J. Mooney and D. A. Weitz, *Adv. Healthcare Mater.*, 2015, **4**, 1628–1633.
- 42 J. Beegle, K. Lakatos, S. Kalomoiris, H. Stewart, R. R. Isseroff, J. A. Nolta and F. A. Fierro, *Stem Cells*, 2015, **33**, 1818–1828. 55

- 1 43 I. Barde, P. Salmon and D. Trono, *Curr. Protoc. Neurosci.*, 2010, ch. 4, unit 4.21.
- 44 M. Geraerts, S. Willems, V. Baekelandt, Z. Debyser and R. Gijssbers, *BMC Biotechnol.*, 2006, **6**, 34.
- 5 45 Y. Morimoto, W. H. Tan, Y. Tsuda and S. Takeuchi, *Lab Chip*, 2009, **9**, 2217–2223.
- 46 P. Agarwal, S. Zhao, P. Bielecki, W. Rao, J. K. Choi, Y. Zhao, J. Yu, W. Zhang and X. He, *Lab Chip*, 2013, **13**, 4525–4533.
- 47 J. M. Zuidema, C. J. Rivet, R. J. Gilbert and F. A. Morrison, *J. Biomed. Mater. Res., Part B*, 2014, **102**, 1063–1073.
- 10 48 H. J. Kong, D. Kaigler, K. Kim and D. J. Mooney, *Biomacromolecules*, 2004, **5**, 1720–1727.
- 49 S. C. Neves, D. B. Gomes, A. Sousa, S. J. Bidarra, P. Petrini, L. Moroni, C. C. Barrias and P. L. Granja, *J. Mater. Chem. B*, 2015, **3**, 2096–2108.
- 15 50 F. R. Maia, K. B. Fonseca, G. Rodrigues, P. L. Granja and C. C. Barrias, *Acta Biomater.*, 2014, **10**, 3197–3208.
- 51 B. H. Lee, B. Li and S. A. Guelcher, *Acta Biomater.*, 2012, **8**, 1693–1702.
- 20 52 A. W. Chan and R. J. Neufeld, *Biomaterials*, 2009, **30**, 6119–6129.
- 53 B. Zhu and H. Yin, *Bioengineered*, 2015, **6**, 125–131.
- 54 M. E. Kidd, S. Shin and L. D. Shea, *J. Controlled Release*, 2012, **157**, 80–85.
- 25 55 F. F. da Cunha, L. Martins, P. K. Martin, R. S. Stilhano, E. J. Paredes Gamero and S. W. Han, *Cytotherapy*, 2013, **15**, 820–829.
- 56 R. H. Kutner, X. Y. Zhang and J. Reiser, *Nat. Protoc.*, 2009, **4**, 495–505.
- 30 57 G. Skjåk-Bræk, H. Grasdalen and O. Smidsrød, *Carbohydr. Polym.*, 1989, **10**, 31–54.
- 58 J. M. Sonego, P. R. Santagapita, M. Perullini and M. Jobbagy, *Dalton Trans.*, 2016, DOI: 10.1039/C6DT00321D.
- 59 J. L. Drury, R. G. Dennis and D. J. Mooney, *Biomaterials*, 2004, **25**, 3187–3199.
- 60 S. J. Bidarra, C. C. Barrias, K. B. Fonseca, M. A. Barbosa, R. A. Soares and P. L. Granja, *Biomaterials*, 2011, **32**, 7897–7904.
- 61 M. M. Segura, A. Kamen and A. Garnier, *Biotechnol. Adv.*, 2006, **24**, 321–337.
- 62 F. Higashikawa and L.-J. Chang, *Virology*, 2001, **280**, 124–131.
- 10 63 K. Ye, H. K. Dhiman, J. Suhan and J. S. Schultz, *Biotechnol. Prog.*, 2003, **19**, 538–543.
- 64 Y. V. Griko, *Biophys. Chem.*, 1999, **79**, 117–127.
- 65 M. A. Croyle, S. M. Callahan, A. Auricchio, G. Schumer, K. D. Linse, J. M. Wilson, L. J. Brunner and G. P. Kobinger, *J. Virol.*, 2004, **78**, 912–921.
- 15 66 C. J. Kearney, H. Skaat, S. M. Kennedy, J. Hu, M. Darnell, T. M. Raimondo and D. J. Mooney, *Adv. Healthcare Mater.*, 2015, **4**, 1634–1639.
- 67 B. Amsden, *Macromolecules*, 1998, **31**, 8382–8395.
- 20 68 M. Grassi, C. Sandolo, D. Perin, T. Coviello, R. Lapasin and G. Grassi, *Molecules*, 2009, **14**, 3003–3017.
- 69 C. Nam-Joon, E. Menashe, X. Anming, L. Wonjae, C. Eric, B. Julie, W. F. Curtis and S. G. Jeffrey, *Biomed. Mater.*, 2009, **4**, 011001.
- 25 70 R. M. Padmashali and S. T. Andreadis, *Biomaterials*, 2011, **32**, 3330–3339.
- 71 Q. Wen, A. Basu, P. A. Janmey and A. G. Yodh, *Soft Matter*, 2012, **8**, 8039–8049.
- 30 72 L. W. Chan, H. Y. Lee and P. W. S. Heng, *Carbohydr. Polym.*, 2006, **63**, 176–187.

35

35

40

40

45

45

50

50

55

55